SEISMIC VULNERABILITY ASSESSMENT OF MODULAR STEEL BUILDINGS

C.D. Annan, M.A. Youssef[1], M.H. El Naggar

Department of Civil and Environmental Engineering, The University of Western Ontario, London, ON, N6A 5B9. CANADA

ABSTRACT

Contemporary seismic design is based on dissipating earthquake energy through significant inelastic deformations. This study aims at developing an understanding of the inelastic behaviour of braced frames of modular steel buildings (MSBs) and assessing their seismic demands and capacities. Incremental dynamic analysis is performed on typical MSB frames. The analysis accounts for their unique detailing requirements. Maximum inter-storey drift and peak global roof drift were adopted as critical response parameters. The study revealed significant global seismic capacity and a satisfactory performance at design intensity levels. High concentration of inelasticity due to limited redistribution of internal forces was observed.

Keywords: Modular steel building, braced frame, earthquake ground motions, incremental dynamic analysis, seismic demand and capacity, ductility, maximum inter-storey drift.

[1] Corresponding author. Tel.: +1 519 661-2111 Ext. 88661; Fax: +1 519 661-3779.
E-mail address: youssef@uwo.ca (M.A. Youssef)

1.0 Introduction

The seismic response of a structural building system depends on several factors including its configuration and dynamic characteristics, and the characteristics of the applied earthquake ground motion. It is imperative to simulate these factors as close to reality as possible in order to correctly predict seismic performance or vulnerability of a given structural system using experimental and/or analytical techniques. Uncertainties and randomness inherent in many of these factors pose a serious challenge in the analysis procedure, especially when the response is largely inelastic. This requires incorporating these uncertainties in the modeling and analysis of the building frame as well as in the definition of structural demand and capacity. Dynamic inelastic analysis is the preferred choice for assessing the seismic capacity of building structures, since realistic and reliable estimates of both force and deformation demands at various locations of the structural system can be obtained.

Inelastic characteristics such as energy dissipation and strength degradation largely affect structural vulnerability under seismic loading. For instance, building systems with large energy dissipation capacity are likely to undergo significantly greater inelastic deformations than systems with relatively limited energy dissipation capacity. In modern design codes, building systems are expected to deform well into the inelastic region under severe earthquakes. The forces resulting from the idealized elastic response spectra, representing site seismicity, are reduced by a force modification or response behaviour factor, R. This factor is also used to amplify the calculated elastic drift which provides an assessment of the potential seismic damage. Drift limits are generally based on storey height of the building frame. The R factor is generally specified for a typical frame configuration and is partly attributed to system's ductility, and partly to the increase in strength beyond design strength as a result of strain hardening of

steel, design assumptions, and internal force redistribution in the inelastic range of response. In the National Building Code of Canada [NBCC, 2005], the R factor is the product of the ductility-related force modification factor, R_d, and the overstrength-related force modification factor, R_o. Selecting appropriate values for these factors to estimate the seismic design base shear and to assess the structural drift demand is an essential step in the design process.

Modular steel building (MSB) systems differ significantly from their traditional onsite counterpart in terms of detailing requirements and method of construction. This building system has been typically used for one-to-six storey schools, apartments, hotels, correctional facilities, dormitories and other similar buildings where repetitive units are required. A detailed description of the MSB technique highlighting its advantages, application and unique detailing requirements has been presented in earlier articles [Annan et al., 2005; Annan et al., 2007; Annan et al., 2008; Annan et al., 2009a]. The technique involves the design of buildings, which are built and finished at one location and transported to be used at another. The finished units/modules of a MSB are connected both horizontally and vertically on-site. Typical details of the MSB system, including the horizontal and vertical connections of different modular units have been described by Annan et al. [2007, 2009a]. Lateral stability of the entire MSB is achieved by adding diagonal braces. Currently, there have been very limited studies on the seismic performance of modular steel building braced systems and their design follows procedures for conventional steel braced frame. The conventional braced frame design provisions generally treat the various brace configurations the same.

The inelastic characteristics of the MSB braced system under severe ground motions may differ significantly from those of regular steel building systems. Fig. 1 shows a typical plan and sections of a MSB. In terms of structural configuration and detailing requirements, the following

specific features distinguish the MSB braced frame from a regular steel braced frame: (1) the existence of ceiling beams (CB) and ceiling stringers (CS) in the MSB frame system may result in natural periods and mode shapes different from those of conventional systems. The floor beams are either set directly on the ceiling beams, as shown in the sections of Fig. 1, or at a specified clearance to allow installation of fire protective layers; (2) brace members in a typical modular steel frame do not intersect at a single working point which may lead to high seismic demands on the vertical connection (VC) between different modular units; (3) all beam-to-column and beam-to-beam connections are achieved using direct welding of the members, unlike in regular frames where clip angles are shop-welded to one member and field-bolted to the other; (4) the Horizontal Connections (HC) of separately finished modules, shown in section A-A, are achieved by field-bolting of clip angles which are shop-welded to the floor beams, (5) the vertical connection (VC) between modular units, shown in section B-B, typically involves partial welding of columns of lower and upper modules and this may lead to independent upper and lower rotations at the same joint. Column continuity has been known to contribute effectively in preventing soft-storey response in multi-storey structures [Tremblay, 2000]. Discontinuity of columns coupled with a possible high seismic demand on the vertical connection of different modules could render inter-storey drifts critical in the design and performance of modular buildings under earthquake ground motions. Proper design of MSB systems is also essential as the system may inherently possess very limited capacity to redistribute internal forces between stories and may be prone to early brace buckling leading to large storey drifts and excessive ductility demands during severe earthquakes.

The present study focuses on quantifying seismic inelastic demands and capacities at the structure level for 2-, 4-, and 6-storey MSB braced frames located in Vancouver and designed for

moderate ductility according to Canadian standards. The behaviour and response of these structures were examined by subjecting representative nonlinear analytical models of the frames to an ensemble of 20 earthquake ground motions scaled to different intensity levels. The spectral acceleration at the structure's fundamental mode period was used to scale each record, thus allowing a reduction in record-to-record variability. The corresponding peak ground acceleration (PGA) was also used as a seismic hazard representation for comparison, in order to determine the more consistent intensity measure for the MSB braced frame system.

Results of a nonlinear static analysis (pushover analysis) in an earlier study [Annan et al., 2009a] were used to identify behaviour characteristics of the selected frames that cannot be obtained from time history analysis but are important in understanding and rationalizing the dynamic response. Particularly, the effect of design philosophy on nonlinear behaviour of MSB braced frames was studied. In the present study, the influence of ground motion intensities and number of stories on maximum inter-storey and global drift demands as well as on maximum inelastic force demands were assessed. The heightwise distribution and record-to-record variability of the maximum inter-storey drift demands were also studied. The drift behaviour provided an assessment of the ductility demands and capacity of the selected MSB braced frames.

2.0 Selection and Design of MSB system

Three heights of a typical modular dormitory building were selected for the nonlinear time history analysis. The same frame configurations were selected and used in an earlier study [Annan et al., 2009a] of nonlinear behaviour of MSB braced frames using nonlinear static analysis. Fig. 2 shows a typical floor plan of the selected buildings and the elevation of the 4-

storey MSB braced frame. Each story is made up of six modules, labelled M#1 to M#6, comprising twelve individual rooms and a corridor. A floor system of a typical modular unit is composed of two floor beams, eleven floor stringers, and a metal deck with concrete composite floor. Similarly, the ceiling framing includes two ceiling beams and a number of ceiling stringers. A clearance of 150 mm was allowed between floor beams and ceiling beams. The composite floor within a modular unit was assumed to be rigid in-plane. The corridor on each floor runs through the middle area of all the modular units, between the two interior columns. The corridors are without ceiling beams to allow mechanical and electrical ducts to run along them.

The lateral response of the building frames in the N-S direction is considered in this study. The lateral force resisting system in this direction is composed of two identical external X-braced frames as shown by the dashed lines within units M#1 and M#6 in Fig. 2. The combined behaviour of the composite floor of the modules and the horizontal connections between these modules is designed to be sufficiently rigid to transfer lateral loads between the modular floor units and to the braced frames. In these frames, the braces are connected to the floor beam-to-column and ceiling beam-to-column joints in each storey/module. Brace connections to the modular framing system are composed of gusset plates welded to the braces.

The design of the selected MSB system has been described extensively by Annan et al. [2009a]. When designing the MSB braced frame, frame members were initially sized on the basis of traditional strength and stiffness design criteria for the specified imposed gravity and earthquake actions. The section sizes of braces, columns, floor beams, roof beams, and ceiling beams obtained from the strength design were evaluated and modified, as necessary, according to ductility design requirements and capacity design procedures. Both the strength and ductility

designs were based on the Canadian standard, CAN/CSA-S16.1-01 [CSA, 2001]. The dead load (DL) from a typical floor was composed of the weights of the concrete floor, an all round metal curtain wall system and insulation, a steel deck and the self-weight of the frame members. Superimposed dead load of 0.75, 0.32, and 0.7 kN/m^2 were applied to account for additional loads on floor, roof, and ceiling, respectively. The live loads (LL) used for the design are based on the NBCC [2005] and are 1.9 kN/m^2 for the individual rooms and 4.8 kN/m^2 for the corridor. A snow load of 1.0 kN/m^2 was assumed for the roof. The seismic loading on each frame was based on the National Building Code of Canada [NBCC, 2005] for the city of Vancouver (Western Canada). Table 1 shows frame member sections obtained from both the strength and ductility designs of the selected MSB buildings.

In the ductility design of frame column members, both the direct summation (DS) and the Square Root of the Sum of the Squares (SRSS) force accumulation approaches [Khatib et al., 1988; Redwood and Channagiri, 1991] were used to estimate brace induced column actions. The use of the SRSS approach is explained by the assumption that in a multi-storey braced frame, all bracing members along the height would not reach their ultimate capacities simultaneously. This assumption has been found to be reasonably conservative for regular braced frames. For MSB braced frames, however, it was observed in a nonlinear static pushover analysis [Annan et al., 2009a] that the use of columns obtained using the DS brace induced force accumulation approach yields the desired response based on the design philosophy. Thus, only column sections resulting from the use of the DS force accumulation approach were utilized in the time history dynamic analysis.

The design philosophy is based on the assumption that columns, beams and brace connections within the structure must be able to resist the resulting induced forces when braces

reach their ultimate strength. For that purpose, the ultimate strength of brace members was taken as the nominal resistance. The brace end connections were thus designed to support the brace nominal tensile strength, A_gF_y. For the beams, the effect of redistribution of loads due to brace buckling or yielding was considered. Beams were thus designed as beam-columns, with the design moment resulting from tributary gravity loads and the axial compression coming from unequal capacity of braces in tension and compression. The design of the vertical welded connections of units of the MSB braced frame was based on traditional elastic method and it accounted for eccentric loading resulting from partial welding of connected columns.

3.0 Analytical Model of MSB frames

Nonlinear analysis requires modeling of the complete load-deformation (or moment-curvature) characteristics of each component of the structure. Generally, a model that represents the essential characteristics of all basic elements is intrinsic to understanding the response of the structure. In this study, one of the two identical external braced frames in each building was modeled as a two-dimensional frame supporting half the building mass. A basic centerline model of the bare MSB braced frame was used with floor, ceiling and roof beams, columns and braces extending from centerline to centerline. Each floor was assumed to behave as a rigid plate. The mass representation was via lumped mass matrices. The damping exhibited by the structure was modeled using the traditional Rayleigh damping model proportional to the initial stiffness matrix. The commonly used householder QR algorithm was utilized for the eigenvalue analysis to compute the natural frequencies and mode shapes of free vibration.

An elasto-plastic material model for steel was employed with a yield stress of 350 N/mm^2, and an elastic modulus of 200 kN/mm^2. An inelastic steel beam-column frame element

was used to represent column members in all modules. A one component beam element was used for all beam representations. These elements account for geometric and material non-linearities. The inelastic behaviour of both the beam and the beam-column elements follows the concept of the Giberson one-component model [Sharpe, 1974], which has a plastic hinge possible at one or both ends of the elastic central length of the member.

During a strong earthquake, a brace member in a concentrically braced frame will be subjected to large inelastic deformations in cyclic tension beyond yield and compression into the post-buckling range. The post-elastic compression is accompanied by significant degradation in compressive resistance after a few cycles of loading [Jain and Goel, 1978]. The Remennikov steel brace member hysteresis [Remmennikov and Walpole, 1997] was used to represent all bracing members. This hysteresis model represents the out-of-plane buckling of the steel brace member but essentially captures the inelastic behaviour under alternate axial tension and compression. The member only permits this hysteresis in the axial component; it is assumed generally to be bi-linear in flexure.

Fig. 3 shows a schematic representation of the vertical connection of modular units. Rigid end blocks (shown by bold lines J1-J2, J2-J3, J2-J4, J5-J6, J6-J7, J6-J8) were provided at the end regions of the beam-column joints within the tube column sections to capture the rigidity of these connection regions. The ends of brace members were also modeled by rigid end blocks to simulate the rigid behaviour expected from the gusset plates. The short column segment between the bottom flange of the floor beam and top flange of the ceiling beam was represented by a vertical inelastic beam-column frame element, M1, whose height represents the clearance between the two beams. This vertical element was pinned internally into a common joint with the

upper unit column, J4, such that an independent upper and lower module rotation would develop at this common joint.

In order to validate the analytical model adopted in the study, an experimental evaluation of the hysteretic characteristics of modular steel braced frames under reversed cyclic loading was carried out [Annan et al., 2009b]. The MSB test specimen consisted of a one-storey, one-bay X-braced panel with tubular brace cross-section, extracted and scaled from the four-storey MSB braced frame. Fig. 4 shows a comparison of the experimental results and the analytical prediction, suggesting that the analytical modeling technique adopted in the present study is capable of predicting the seismic behavior of MSB braced frames.

4.0 Selection of Ground Motion Records and Analysis Characteristics

Most seismic design codes and recommendations specify seismic hazard in terms of a single intensity measure such as the peak ground acceleration (PGA) or a spectral ordinate at a given period. In the NBCC [2005], the seismic hazard is described by spectral-acceleration values at periods of 0.2, 0.5, 1.0 and 2.0 seconds. Spectral acceleration is a measure of ground motion that takes into account the sustained shaking energy at a specific period. For the selected site of the selected modular buildings, the 2% in 50 year intensities of ground motion (expressed as spectral accelerations, $S_a(T)$, that correspond to fundamental periods of the building frames) were evaluated as 0.96g, 0.85g, and 0.75g for the 2-, 4-, and 6-storey frames respectively.

It is well known that different ground motion records scaled to the same PGA do not induce the same level of response in, and do not cause the same amount of damage to a given structure. This is due to variation in other seismic hazard parameters such as frequency content, event duration and effective number of loading cycles. Hence, the response obtained using one

ground motion may not provide sufficient confidence that the structure will yield similar response if subjected to another ground motion record with the same PGA. Shome and Cornell [1999] showed that sufficient accuracy can be obtained in the estimation of seismic demands of mid-rise buildings if ten to twenty ground motion records are considered. FEMA [2000a] recommends selecting a suite of 10 to 20 accelerograms representative of the site and hazard level to achieve the collapse prevention level.

Vamvatsikos and Cornell [2004] compiled and used a scenario earthquake comprising of 20 historical ground motion records from three earthquakes (i.e. 1979 Imperial Valley; 1987 Superstition Hills; and 1989 Loma Prieta) to analyze mid-rise buildings. The records selected belong to a bin of relatively large magnitudes, 6.5 – 6.9, and moderate epicentral distances in the range of 15-32 km. All of the accelerograms were recorded on firm soil and bear no marks of directivity. This study adopted the same ensemble of ground motion records; they are obtained from the PEER strong motion database and their characteristics are listed in Table 2.

The seismic inelastic demands of the selected building systems were determined using the incremental dynamic analysis (IDA) procedure. IDA was developed by Luco and Cornell [1998] and has been described in detail in Vamvatsikos and Cornell [2002] and Yun et al. [2002]. This analysis technique has also been incorporated in modern seismic design recommendation [FEMA, 2000a]. The IDA requires a series of nonlinear response history analyses of a modeled structure for an ensemble of ground motions, each scaled to many intensity levels. Intensity levels are selected to cover the entire range of structural response, from elastic behavior through yielding to dynamic instability (or until a limit state “failure” occurs). From the results of these multiple analyses, statistics on the variation of demand and capacity with ground motion character can be evaluated to summarise the results.

Estimating seismic demand with sufficient accuracy requires selection of efficient analysis characteristics. Shome et al. [1998] observed that by scaling ground motion records to the target spectral acceleration at the fundamental-mode period of a structure, seismic demands at this intensity can be efficiently estimated. The spectral acceleration at 5% damping, $S_a(T_1, 5\%)$, was primarily used as intensity measure (IM) in this study. The simple stepping algorithm [Vamvatsikos and Cornell, 2002] was used to scale ground motion records. Demand distribution with Peak Ground Acceleration, PGA, was also studied in order to compare dispersion of response parameters, and consequently to assess the most efficient intensity measure parameter for the MSB system within the entire response spectrum.

Seismic behavior can be measured using fracture life, energy dissipation capacity, maximum drift and ductility capacity, etc. Maximum inter-storey drift is often used as a primary damage intensity parameter in the vulnerability assessment of moment resisting frames but have also been used to characterize global dynamic response of ductile concentrically braced frame structures [Sabelli, 2001; Uriz and Mahin, 2004]. The maximum (over all stories) peak inter-storey drift ratio (θ_{max}), and peak roof drift ratio (θ_{roof}) were selected as global Demand Parameters (DP) to study the structural response of the selected frames during the ground motions duration. The inter-storey drift ratio was computed as the difference in displacements of adjacent stories divided by the inter-storey height, and the peak roof drift ratio is obtained from the ratio of the peak roof drift during the duration of the ground motion to the overall height of the structural frame. The IDA curves were then obtained for each record from a plot of demand parameters against their corresponding intensity measure parameters.

5.0 Evaluation of Seismic Inelastic Response Characteristics

5.1 Eigenvalue Analysis

To evaluate the seismic vulnerability of MSB frames using inelastic dynamic analyses, an assessment of their dynamic response characteristics is necessary. Modal or eigenvalue analyses were conducted for the 2-, 4- and 6-storey MSB braced frames to find the frequencies and mode shapes of free vibration. Essentially, the behavior of these frames was dominated by their first-mode but there was some sensitivity to higher modes. Table 3 shows the first and second-mode periods and mass participation factors for the selected frames. It also shows the empirical estimate of design periods based on the NBCC [2005]. Shorter empirical design periods would result in the provision of greater base shear capacities to the structures, which is the case for the 4- and 6-storey MSB frames.

5.2 Results of Incremental Dynamic Analysis

Results of a total of about 2500 nonlinear time history analyses, conducted on the three nonlinear analytical models of the MSB braced frame for the selected ground motion records, were plotted as IDA curves and are shown in Figs. 5 to 8. In each plot, a structural Demand Parameter (DP) resulting from a scaled ground motion record of a known Intensity Measure (IM) provided a single point. Similar responses which correspond to different values of IM for the same ground motion record provided other points that joined together to produce a spline fit of the IDA curve for that record and selected frame model. Thus, for the three selected MSB braced frames under the suite of 20 ground motion records, a total of 60 IDA curves were generated for a specified IM versus DP. In Figs. 5 and 6, the ground motion IM was the 5% damped spectral acceleration of the scaled ground motion at the fundamental mode period of the structure, $S_a(T_1$,

5%). The engineering DP in these plots were respectively the maximum (over all stories) peak inter-storey drift ratio, θ_{max}, and the peak roof drift ratio, θ_{roof}, expressed as a percentage. These demand parameters were also plotted against corresponding PGA of the scaled ground motion records in Figs. 7 and 8, respectively. These IM versus DP combinations used in this study resulted in an overall total of 240 IDA curves.

The variety and dispersion of the results obtained for different ground motions and different frame heights as shown by these curves is remarkable. All curves, however, exhibit a distinct linear elastic behavior before the first sign of significant nonlinearity occured. Comparing Figs. 5 and 6 against Figs. 7 and 8 it is observed in the linear elastic response range that, the $S_a(T_1, 5\%)$ is a more consistent intensity measure than the PGA. The elastic 'stiffness' (defined here as the ratio of the intensity measure to the demand parameter in the linear elastic range of response) varies from record to record when PGA is used as an intensity measure (Figs. 7 and 8). On the other hand, the $S_a(T_1, 5\%)$ provided almost the same elastic 'stiffness' across records. Smaller dispersion of the demand parameter for a given intensity measure implies that an efficient prediction of demand can be made with a smaller sample of records and hence a fewer non-linear time history analyses.

Based on the above observation, it can be inferred that the $S_a(T_1, 5\%)$ is a more suitable intensity measure for the MSB braced frames and would subsequently be adopted as the primary intensity measure in the demand and capacity assessment of the selected frames. It can also be observed in the linear elastic range of response that, the dispersion across records is smaller in the 2-storey MSB braced frame than the 6-storey frame because the former exhibits more resemblance to a SDOF system by the dominance of its first mode. The magnitude of the elastic 'stiffness' is dependent on the period of the structure. Based on the plot of $S_a(T_1, 5\%)$ versus

θ_{max}, the average elastic 'stiffness' was estimated as 4.0, 1.8, and 1.25 (in units of g over %) for the 2-, 4-, and 6-storey MSB braced frames respectively. For all three frames, the first brace buckling occurred at θ_{max} of about 0.33%.

In the inelastic range of response, the IDA curves are generally dissimilar, some displaying a softening behavior with a gradual degradation towards collapse and others displaying a weaving behavior indicative of 'excessive hardening' and 'softening' of the structure. Generally, these curves indicate a non-monotonic relation between demand parameters and intensity measures for reasons as discussed below.

The demand parameter by definition is non-differentiable It contains absolute values of maximum responses of the time history analyses. These maxima may occur at different time instants. In addition, scaling the records as well as the pattern and timing of the ground motion excitation may alter the properties of the structure as it is subjected to different intensity levels at different times. At a lower intensity, the frame may deform significantly in one direction due to a strong pulse occurring at a later stage of the ground motion record. If the intensity of the same record is increased, an earlier pulse may be strong enough to deform the frame in the opposite direction and this may change its dynamic characteristics, protecting it from the effect of the later stronger pulse. Inelastic drifts may also occur disproportionately in one lateral direction depending on the characteristics of the excitation and asymmetry between the tensile capacity and buckling resistance of the braces.

In general, a stiffer braced frame would experience a significant change in its dynamic properties after brace buckling. Because of the sensitivity of inter-storey drift to brace buckling, such frames are likely to produce a more complex IDA curves than would be expected for a ductile moment resisting frame, say.

Finally, for MSB braced frame, redistribution of internal forces from one storey to another may be more limited due to limited alternative load paths. Consequently, a concentration of inelasticity may occur in one level over the height of the frames. This may further exaggerate the phenomena and complexity as described above.

Although each of the IDA curves is a defined deterministic entity, the inherent random variability with ground motion record type requires a statistical assessment of demand. The IDA curve set under the suite of ground motions were summarised by defining the 16%, 50%, and 84% IDA curves [Vamvatsikos and Cornell, 2002; Vamvatsikos and Cornell, 2004; Vamvatsikos and Cornell, 2005; Han and Chopra, 2006]. This summary technique enabled compression of the enormous data to a probabilistic distribution of a demand parameter given an intensity measure. Moreover, engineering design is often based on either the median, mean or 84th percentile. The fractile curves were obtained by computing the 16%, 50%, and 84% fractile values of the demand parameters, θ_{max} and θ_{roof}, for a given ground motion intensity measure, $S_a(T_1, 5\%)$. Figs. 9, 10, and 11 show the 16%, 50%, and 84% fractile IDA curves for the 6-, 4-, and 2-storey MSB braced frames. Such fractile curves can be combined with a probabilistic seismic hazard analysis to produce mean annual frequencies of exceeding defined limit states.

The fractile IDA curves can also represent seismic demand curves of the frames and may be used to assess their performance by comparing with allowable drift demands at any given intensity and probability level. For example, given the design level ground motion intensity of $S_a(T_1, 5\%) = 0.75g$ at the 2% in 50 year probability level for the 6-storey MSB frame, 16% of the records would produce $\theta_{max} \leq 0.62\%$, 50% would produce $\theta_{max} \leq 0.79\%$, and 84% of the records would yield $\theta_{max} \leq 1.15\%$. For the 4-storey MSB frame at its design level intensity of $S_a(T_1, 5\%) = 0.85g$, 16% of the records would produce $\theta_{max} \leq 0.46\%$, 50% of the records would yield $\theta_{max} \leq$

0.51%, and 84% of the records would yield $\theta_{max} \leq 0.73\%$. For the 2-storey MSB frame at the design level intensity of $S_a(T_1, 5\%) = 0.96g$, 16% of the records would produce $\theta_{max} \leq 0.22\%$, 50% of the records would yield $\theta_{max} \leq 0.23\%$, and 84% of the records would yield $\theta_{max} \leq 0.24\%$. The above probabilistic drift demands of the 2-storey MSB frame are essentially within its elastic response range. In the NBCC [2005], drift limits are based on the median 2% in 50 year seismic hazard level and are given as 1% for post-disaster buildings, 2% for high importance buildings, and 2.5% for other buildings. Hence, the use of median ground motions for these frames would yield satisfactory performance in any building category.

5.3 Inelastic Distribution along Height of MSB Frame

Acute lateral drifts on the weak stories of a building may give rise to severe structural damage or even cause structural collapse. Multi-storey braced frames typically exhibit large variations in storey drift and inelastic demand over their height when subjected to strong ground motions [Perotti and Scarlassara, 1991; Tremblay and Robert, 2001; Martinelli et al. 2000]. This is mainly due to the degradation in brace compressive resistance that results from a number of cycles of inelastic excursions and successive compression load cycles beyond brace buckling. The storey shear resistance diminishes at levels where brace buckling occurs first, promoting the development of larger storey drifts at these floors and consequently the formation of storey mechanism. Their limited capacity to redistribute the inelastic demand over the height of a building increases their vulnerability. Inelastic drifts may also occur disproportionately in one lateral direction (depending on the characteristics of the excitation) owing to the asymmetry between the tensile capacity and buckling resistance of the braces.

Lateral drift is considered a system design criterion that would require consideration of all structural elements and components in the building system. As mentioned earlier and also shown in Fig. 2, one of the important features that distinguish an MSB braced frame from a regular braced frame is the incorporation of ceiling beams in the former. These beams also serve as horizontal members for brace upper end connections in each modular unit. The vertical connections of different modular units is such that columns are not continuous over two consecutive vertical units, with some clearance allowed between ceiling beams of a lower modular unit and floor beams of an upper unit. The behaviour of this configuration and the vertical connections of modular units may result in independent rotation of upper and lower module columns at the same joint. This may influence the definition of inter-storey drift for this frame system and consequently affect its inelastic demands (including P-delta effect) especially after brace buckling. Furthermore, this unique configuration may present additional limitation on the redistribution of internal forces from one modular unit to another, which may lead to a concentration of inelasticity in one level over the height of the frames.

In the IDA plots and summaries presented above, inter-storey drift was evaluated as the difference in displacements at floor beam levels of consecutive modular units, ignoring any influence due to ceiling beam between these floor beams. The peak inter-storey drift angle at a floor level during a ground motion event may change (either increase or decrease) at the ceiling level within the same modular unit, thus altering the distribution of lateral deformation over the height of the frame. Figs. 12, 13 and 14 examine the inter-storey drift distribution taking into account the presence of ceiling beam levels. In these figures, heightwise distributions of peak floor-to-ceiling and peak ceiling-to-floor drifts (accounting for ceiling beam level drifts) in the 6-, 4-, and 2- storey MSB frames for the ground motion recorded at El Centro Array #13 during the

1979 Imperial Valley earthquake (see No. 14 in Table 2) are compared with inter-storey drifts as defined above at three different intensity levels: $S_a(T_1, 5\%)$ = 0.2g, 1.7g, and 2.0g for the 6-storey frame; $S_a(T_1, 5\%)$ = 0.3g, 2.0g, and 3.0g for the 4-storey frame; $S_a(T_1, 5\%)$ = 0.4g, 2.5g, and 4.0g for the 2-storey MSB frame.

The behaviour observed under the selected earthquake record above is found to be representative of the response under all the other selected ground motion records and the intensity levels selected produced responses that represent both elastic and inelastic responses of the MSB frames. The figures demonstrate that within the entire range of structural response of the three building heights considered in the study, floor-to-floor inter-storey drifts can satisfactorily represent inter-storey drift demand without explicitly considering the ceiling beam levels. The inelastic range of response is more affected by the presence of ceiling beam levels, especially at the location of maximum inter-storey drift (lower level), but this effect is insignificant. In this range of response, the inter-level drift angle between the ceiling beam and floor beam levels at maximum inter-storey drift regions are slightly lower than the inter-storey drift angle between floor-to-floor beam levels. In the elastic range of response, i.e. at lower ground motion intensities, there is almost no variation in this drift angle.

Figs. 15, 16, and 17 display a storey-to-storey profile of the peak inter-storey drift ratios at different intensity, $S_a(T_1, 5\%)$, levels for the selected ground motion accelerograms. Fig. 18 shows the median peak inter-storey drift ratios over the selected ground motion records at some selected ground motion intensities that produced both elastic and inelastic responses. In general, distribution of inter-storey drift along the height of the MSB braced frames becomes non-uniform with increasing intensity of ground motion, concentrating at specific stories. In the elastic range of response (Figs. 15a, 16a, and 17a), the storey level experiencing maximum drift

varies from record to record. The upper storey levels are mostly affected in this response range: For the 6-storey MSB braced frame, the 3rd to 5th storey levels experience maximum inter-storey drifts for different ground motion records; The 3rd storey level is almost solely affected in the 4-storey MSB frame; For the 2-storey, the maximum inter-storey drift occurred in the 1st storey level for all the ground motion records. In the post-elastic range of response, distribution of inter-storey drift demand varies from record to record in terms of amplitude but follows a very similar pattern for a given modeled frame. Also, a similar trend is maintained as the ground motion intensity increases within the inelastic range of response. Clearly, in this response range, there is a very high concentration of inelasticity in mainly the 1st storey level for all the frame heights considered.

5.4 Structural Drift Demand and Capacity of MSB Braced frame

Each of the IDA curves illustrates the demand imposed on the modeled MSB frame structure by a specified ground motion record at different intensities. The question of whether inter-storey drift ratio can be used as a primary damage parameter to predict global capacity of MSB braced frames is a rational one. Several local damage events can take place in elements such as gusset plates, bracing members, beams and columns, and in connections including vertical connections of different modular units. However, results from inelastic static (pushover) analyses [Annan et al., 2008] revealed that designing the frames based on the capacity design philosophy restricts global failure mechanism to essentially failure in brace members alone. Meanwhile, beams, columns and brace connections are shielded from premature inelastic failure. Because of the sensitivity of inter-storey drift to brace buckling (i.e. failure of braces are more evident in maximum inter-storey drift) and the tendency for concentration of inelastic effects

within a storey of a MSB system, the peak inter-storey drift can relate well to both global and local storey collapse. Thus, it can be used as a reasonable damage measure.

Clearly, the global system dynamic capacity would vary from record to record. For a single IDA curve, either an intensity-based or a demand-based limit state or even both can be useful in defining the global collapse capacity [Vamvatsikos and Cornell, 2002]. In general, the demand-based limit states are known to be useful for defining performance levels other than structural collapse, and the intensity-based limits better assess collapse capacity. In the FEMA [2000a] methodology, structural capacity is defined at the point when the rate of increase of the maximum inter-storey drift with increasing ground motion intensity exceeds five times that associated with the initial 'elastic' slope (that is, tangent slope of 20% of elastic slope). Alternatively, it is defined at a prescribed maximum inter-storey drift ratio beyond which the reliability of the analysis is not considered trustworthy (e.g. 10% for collapse prevention of special moment resisting frames). Due to the weaving nature of some of the IDA curves, both the former intensity-based and the latter demand-based limit states may result in more than one capacity point. In such a case, the first capacity point along the IDA curve from the origin is recommended when using the demand-based rule and the final capacity point is recommended for the intensity-based rule [Vamvatsikos and Cornell, 2002]. The 20% tangent slope approach is assumed to be indicative of imminent collapse. Therefore, it is adopted in this study to define global capacity of the MSB braced frames under the selected ground motions.

The global capacity of the MSB braced frames under the selected ground motion records representing the collapse prevention limit state defined by FEMA [2000a] are shown by the open triangular shaped markers on the IDA curves in Fig. 5. Such limit states can also be summarized into their 16, 50, and 84 percentile values as shown on the fractile IDA curves in Figs. 9a, 10a,

and 11a. These points are obtained by determining the capacities individually for each ground motion record and then estimating their fractile values. Table 4 summarises the fractile structural drift capacities in terms of $S_a(T_1,5\%)$ for the selected MSB braced frames. It also shows the standard deviation of the capacities over the selected ground motions based on the assumed lognormal probability distribution [Hamburger et al., 2003]. The median capacities in terms of spectral acceleration associated to the NBCC design drift limit of 2.0% have also been included in this table. It is observed that the median capacities associated to the collapse prevention limit state are in the range of between 1.4 and 2.0 times the median capacities associated to the code's drift limit (and about 3 to 5 times the design intensity levels). Capacity reduction factors have been recommended [FEMA, 2000a] to be applied in the case of ductile moment resisting frames to account for the variability in the computed capacities. Such factors are statistically based and are currently not available for ductile braced frames. The capacities shown in Table 4 are those obtained without explicitly accounting for uncertainties and randomness inherent in their prediction. Table 5 shows the fractile capacities in terms of θ_{max}, including their standard deviations. The median capacities are between 1.6 and 2.6 times the NBCC drift limit for the selected MSB frames.

5.5 Ductility Demand Assessment

Ductility represents the capacity of a structure to dissipate energy and plays an important role in the determination of seismic design forces and evaluation of seismic vulnerability. From the incremental dynamic analyses, IDA curves are constructed with ductility as the engineering demand parameter against the 5% damped spectral acceleration at the fundamental-mode period of the structure, $S_a(T_1, 5\%)$. Fig. 19 shows the ductility demands of the 6-storey, 4-storey and 2-

storey MSB braced frame under the selected ground motion records. This global ductility demand is indicative of the overall deformation of the structure and defined as the average value of the storey ductilities. This definition yields reasonable results for moment resisting frames [Reyes-Salazar, 2002] and is adopted in this study. The storey ductility is defined for each storey as the ratio of the maximum inter-storey drift during the ground motion duration to the maximum inter-storey drift over all stories when plasticization occurs in the structure for the first time. A large variation of ductility demand with frame height and from ground motion record to record is observed.

The ductility demands of the selected frames under the twenty ground motion records are summarized into their 16^{th}, 50^{th}, and 84^{th} fractile curves, as shown in Fig. 20. Ductility capacities are evaluated based on the median capacities in $S_a(T_1, 5\%)$ associated to the NBCC 2.0% drift limit and the collapse prevention level identified in section 5.4 above. Table 6 consists of the ductility capacities obtained for the selected MSB braced frames. These capacities range from 1.8 to 4.8 and increase with decrease in frame height. The configuration of the MSB braced frame, particularly the vertical connections of different modular units, is more effective on the structural response at higher storey levels and this influences the behavior of the entire frame.

6.0 Conclusions

The severity of damage a building suffers depends on its vulnerability and the seismic hazard it is exposed to. Vulnerability is controlled by the overall capacity of the building, which could be a function of the inter-storey drift, plastic rotations, or member forces. Earthquake ground accelerations cause building response resulting in drifts and member forces, all of which can represent demands. If both the ground motion demand and the structure's capacity to resist this

demand could be predicted with some certainty, then buildings could be designed with some level of confidence of performing as desired. In this study an understanding of inelastic effects in modular steel building braced frames under earthquake ground motions is developed. The influence of ground motion intensities and number of stories on maximum drift demands have been assessed. The heightwise distribution and record-to-record variability of maximum drift demands was also studied. The study has also predicted drift and ductility demands given any particular level of ground motion and has estimated the capacities at the collapse prevention level with a corresponding probability that this performance level may not be exceeded. The general conclusions drawn from the results of this study are summarized below:

1. The selected MSB braced frames exhibited predominantly first-mode response but there was some sensitivity to higher modes.
2. At the design level ground motion intensity of all the selected MSB braced frames, the predicted drift demands based on the median ground motions gave satisfactory performance on the basis of the NBCC drift limits.
3. Within the entire range of structural response of the three MSB heights considered in the study, floor-to-floor inter-storey drifts can satisfactorily represent inter-storey drift demand without explicitly considering the effect of drift at the ceiling beam levels.
4. The distribution of inter-storey drift demand along the height of the frames varies from record to record in terms of amplitude but follows a very similar pattern. The upper storey levels generally experience maximum drift demands in the elastic range of response. In the inelastic range of response, there is a high concentration of inelasticity in mainly the 1st storey level. This is due to inelastic behavior of braces and the limited redistribution of internal forces from one storey level to the other.

5. The median capacities in terms of spectral acceleration, $S_a(T_1, 5\%)$, for the collapse prevention drift limit state are in the range of between 1.4 and 2.0 times the median capacities associated to the NBCC drift limit of 2.0%.
6. The median capacities in terms of maximum inter-storey drift based on collapse prevention levels are between 2.0 and 3.3 times the NBCC drift limit.
7. Both drift and ductility demands vary from record to record and with frame height.
8. All three MSB braced frames possess significant ductility capacity of between 1.8 and 2.8 based on the median capacities associated to the NBCC drift limit, and between 3.9 and 4.8 based on the median capacities associated to collapse prevention levels.

Acknowledgements

This research was funded by the National Sciences and Engineering Research Council of Canada (NSERC) and The University of Western Ontario.

References

Annan, C.D., Youssef, M.A. and El-Naggar, M.H. [2005] "Analytical investigation of semi-rigid floor beams connection in modular steel structures," *33rd Annual general conference of the Canadian Society for Civil Engineering,* Toronto, Canada, GC-352.

Annan, C. D., Youssef, M. A. and El-Naggar, M. H. [2007] "Seismic performance of modular steel braced frames," *Proc. of the Ninth Canadian Conference on Earthquake Engineering*, Ottawa, Ontario, Canada.

Annan, C.D., Youssef, M.A. and El-Naggar, M.H. [2008] “Effect of directly welded stringer-to-beam connections on the analysis and design of modular steel building floors,” *Advances in Structural Engineering,* in press, accepted in October 2008.

Annan, C.D., Youssef, M.A**.** and El-Naggar, M.H. [2009a] "Seismic overstrength in braced frames of Modular Steel Buildings," *Journal of Earthquake Engineering*, 13(1), 1-21.

CSA [2001] *Handbook of Steel Construction, 7th Edition*, Canadian Institute of Steel Construction, Willowdale, Ontario, Canada.

Annan, C.D., Youssef, M.A. and El-Naggar, M.H. [2009b] “Experimental evaluation of the seismic performance of modular steel braced frames,” *Engineering Structures,* in press, accepted in February 2009

FEMA [2000a] *Recommended seismic design criteria for new steel moment frame buildings*, FEMA-350, SAC Joint Venture, Federal Emergency Management Agency, Washington, DC.

FEMA [2000b] *Recommended seismic evaluation and upgrade criteria for existing welded steel moment frame buildings*, FEMA-351, SAC Joint Venture, Federal Emergency Management Agency, Washington, DC.

Hamburger, R. O., Foutch, D. A. and Cornell, A. C. [2003] “Translating research to practice: FEMA/SAC performance-based design procedures,” *Earthquake Spectra*, *Special issue: Welded steel moment-frame structures – Post-Northridge* 19(2).

Jain, A.K. and Goel, S.C. [1978] *Hysteresis models for steel members subjected to cyclic buckling or cyclic end moments and buckling – User’s guide for DRAIN-2D: EL9 and EL10*, Report UMEE 78R6, Department of Civil Eng., Univ. of Michigan, Ann Arbour, MI, USA.

Khatib, I.F., Mahin, S.A. and Pister, K.S. [1988] *Seismic behaviour of concentrically braced steel frames*, Report UCB/EERC-88/01, Earthquake Engineering Research Center, University of California, Berkeley, CA, USA.

Luco, N. and Cornell, C. A. [1998] "Effects of random connection fractures on the demands and reliability for a three-story pre-Northridge (SMRP) structure," *Proc. of the sixth U.S. National Conf. on Earthquake Eng*., Earthquake Engineering Research Institute, Oakland, California.

Martinelli, L., Perotti, F. and Bozza, A. [2000] "Seismic design and response of a 14-story concentrically braced steel building," *Proc. STESSA 2000 Conf.*, Montreal, Canada, pp. 327-334.

NBCC [2005] *National Building Code of Canada*, Institute for Research in Construction, National Research Council of Canada, Ottawa, Ontario, Canada.

Perotti, F. and Scalassara, P. [1991] "Concentrically braced frames under seismic actions: Nonlinear behavior and design coefficients," *Earthquake Engineering and Structural Dynamics* 20, 409-427.

Redwood, R.G. and Channagiri, V.S. [1991] "Earthquake resistant design of concentrically braced frames," *Canadian Journal of Civil Engineering* 18(5), 839-850.

Remennikov, A. and Walpole, W. [1997] "Analytical prediction of seismic behaviour for concentrically-braced steel systems," *Earthquake Engineering and Structural Dynamics* 26, 859-874.

Reyes-Salazar, A. [2002] "Ductility and ductility reduction factor for MDOF systems," *Structural Engineering and Mechanics* 13(4), 369-385.

Sabelli, R. [2001] *Research on improving the design and analysis of earthquake-resistant steel-braced frames*, The 2000 NEHRP Professional Fellowship Report, Earthquake Engineering Research Institute, USA.

Shome, N. and Cornell, C.A. [1999] *Probabilistic seismic demand analysis of nonlinear structures*, RMS Report-35, Reliability of Marine structures Group, Stanford University, Stanford.

Shome, N., Cornell, C.A., Bazzurro, P. and Carballo, J. [1998] "Earthquake, records, and nonlinear MDOF responses," *Earthquake Spectra* 14(3), 469-500.

Tremblay, R. and Robert, N. [2001] "Seismic performance of low- and medium-rise chevron braced steel frames," *Canadian Journal of Civil Engineering* 28(4), 699-714.

Tremblay, R. [2000] "Influence of brace slenderness on the seismic response of concentrically braced steel frames," *Proc. STESSA 2000 Conference*, Montreal, Canada, pp. 527-534.

Tremblay, R. [2002] "Inelastic seismic response of steel bracing members," *Journal of Constructional Steel Research* 58, 665–701.

Uriz, P. and Mahin, S. A. [2004] "Seismic Performance assessment of concentrically braced steel frames," *Proc. of the 13th World Conf. on Earthquake Eng.*, Vancouver, Canada, Paper No. 1639.

Vamvatsikos, D. and Cornell, C. A. [2002] "Incremental dynamic analysis," *Earthquake Engineering & Structural Dynamics* 31(3), 491-514.

Vamvatsikos, D. and Cornell, C. A. [2004] "Applied incremental dynamic analysis," *Earthquake Spectra* 20(2), 523-553.

Yun, S., Hamburger, R.O., Cornell, C.A. and Foutch, D.A. [2002] "Seismic performance evaluation for steel moment frames," *Journal of Structural Engineering* 128(4), 534-545.

Table 1. Member sections from strength and ductility designs of MSB braced frame

Number of stories	Frame Member	Storey / Floor #	Strength Design	Ductility Design (column design by SRSS approach)	Ductility Design (column design by DS approach)
2-storey MSB braced frame	Braces	2	HS 89X89X6	HS 89X89X6	
		1	HS 89X89X6	HS 89X89X6	
	Columns	2	HS 89X89X6	HS 127X127X5	
		1	HS 127X127X5	HS 178X178X8	
	Beams	Roof	W100X19	W100X19	
		Floor 2	W100X19	W100X19	
		Floor 1	W100X19	W100X19	
		Ceiling	W100X19	W100X19	
4-storey MSB braced frame	Braces	4	HS 76X76X5	HS 76X76X6	
		3	HS 76X76X5	HS 76X76X6	
		2	HS 89X89X6	HS 89X89X6	
		1	HS 89X89X6	HS 89X89X6	
	Columns	4	HS 76X76X5	HS 102X102X6	HS 102X102X6
		3	HS 178X178X5	HS 178X178X6	HS 178X178X6
		2	HS 178X178X5	HS 203X203X6	HS 203X203X10
		1	HS 178X178X6	HS 203X203X8	HS 254X254X10
	Beams	Roof	W100X19	W100X19	
		Floor 4	W100X19	W100X19	
		Floor 3	W100X19	W100X19	
		Floor 2	W100X19	W100X19	
		Floor 1	W100X19	W100X19	
		Ceiling	W100X19	W100X19	
6-storey MSB braced frame	Braces	6	HS 76X76X5	HS 76X76X5	
		4	HS 102X102X5	HS 102X102X6	
		4	HS 102X102X5	HS 102X102X6	
		3	HS 102X102X5	HS 102X102X6	
		2	HS 102X102X5	HS 102X102X6	
		1	HS 102X102X5	HS 102X102X6	
	Columns	6	HS 89X89X5	HS 102X102X6	HS 102X102X6
		5	HS 127X127X6	HS 178X178X6	HS 178X178X6
		4	HS 178X178X10	HS 178X178X10	HS 203X203X10
		3	HS 203X203X10	HS 203X203X10	HS 305X305X10
		2	HS 254X254X10	HS 254X254X10	HS 305X305X13
		1	HS 305X305X10	HS 305X305X10	HS 305X305X13
	Beams	Roof	W100X19	W100X19	
		Floor 6	W250X33	W250X33	
		Floor 5	W250X33	W250X33	
		Floor 4	W250X33	W250X33	
		Floor 3	W250X33	W250X33	
		Floor 2	W250X33	W250X33	
		Floor 1	W250X33	W250X33	
		Ceiling	W100X19	W100X19	

Table 2. Selected earthquake ground motion records

No.	Event	Year	Record station	Φ[1]	M*[2]	R*[3] (km)	PGA (g)
1	Imperial Valley	1979	Plaster City	45	6.5	31.7	0.042
2	Imperial Valley	1979	Plaster City	135	6.5	31.7	0.057
3	Imperial Valley	1979	Westmoreland Fire Sta.	90	6.5	15.1	0.074
4	Imperial Valley	1979	Westmoreland Fire Sta.	180	6.5	15.1	0.11
5	Imperial Valley	1979	El Centro Array #13	140	6.5	21.9	0.117
6	Imperial Valley	1979	El Centro Array #13	230	6.5	21.9	0.139
7	Loma Prieta	1989	Agnews State Hospital	90	6.9	28.2	0.159
8	Loma Prieta	1989	Coyote Lake Dam	285	6.5	22.3	0.179
9	Superstition Hill	1987	Wildlife Liquefaction Array	90	6.7	24.4	0.18
10	Superstition Hill	1987	Wildlife Liquefaction Array	360	6.7	24.4	0.2
11	Loma Prieta	1989	Sunnyvale Colton Ave	270	6.9	28.8	0.207
12	Loma Prieta	1989	Sunnyvale Colton Ave	360	6.9	28.8	0.209
13	Loma Prieta	1989	Anderson Dam	270	6.9	21.4	0.244
14	Imperial Valley	1979	Chihuahua	282	6.5	28.7	0.254
15	Loma Prieta	1989	Hollister Diff. Array	165	6.9	25.8	0.269
16	Loma Prieta	1989	Hollister Diff. Array	255	6.9	25.8	0.279
17	Imperial Valley	1979	Cucapah	85	6.9	23.6	0.309
18	Loma Prieta	1989	WAHO	0	6.9	16.9	0.37
19	Loma Prieta	1989	Holister South &Pine	0	6.9	28.8	0.371
20	Loma Prieta	1989	WAHO	90	6.9	16.9	0.638

[1] Component, [2] Moment Magnitudes, [3] Closest Distances to Fault Rupture

Source: PEER Strong Motion Database, http://peer.berkeley.edu/svbin

Table 3: Dynamic characteristics of selected MSB braced frames

Dynamic characteristics		MSB Braced frame		
		2-storey	4-storey	6-storey
Period (sec)	NBCC design	0.21	0.35	0.48
	1st mode	0.20	0.42	0.61
	2nd mode	0.08	0.16	0.21
Mass participation factor (%)	1st mode	94	81	77
	2nd mode	5	15	17

Table 4: 16%, 50%, and 84% fractile capacities in terms of intensity measure, $S_a(T_1,5\%)$

MSB frame	Design level intensity, $Sa(T_1)$ in g	Fractile S_a capacity (g) based on collapse prevention level			Standard Dev. of median capacity	S_a capacity (g) based on NBCC drift limit
		16%	50%	84%		
2-storey	0.96	2.50	5.50	10.00	0.61	4.00
4-storey	0.85	1.80	3.30	5.25	0.53	1.75
6-storey	0.75	1.60	2.45	3.75	0.44	1.25

Table 5: 16%, 50%, and 84% fractile capacities in terms of maximum drift, θ_{max}

MSB frame	Fractile θ_{max} capacities (%)			Standard Dev. of capacities
	16%	50%	84%	
2-storey	1.2	4.0	6.9	0.76
4-storey	4.4	6.7	10.0	0.63
6-storey	3.2	6.7	9.8	0.43

Table 6: Ductility capacity based on NBCC drift limit and collapse prevention median capacities in $S_a(T_1,5\%)$

MSB frame	Ductility capacity based on NBCC drift limit median capacity in Sa	Ductility capacity based on collapse prevention level median capacity in Sa
2-storey	2.80	4.80
4-storey	2.40	4.50
6-storey	1.80	3.90

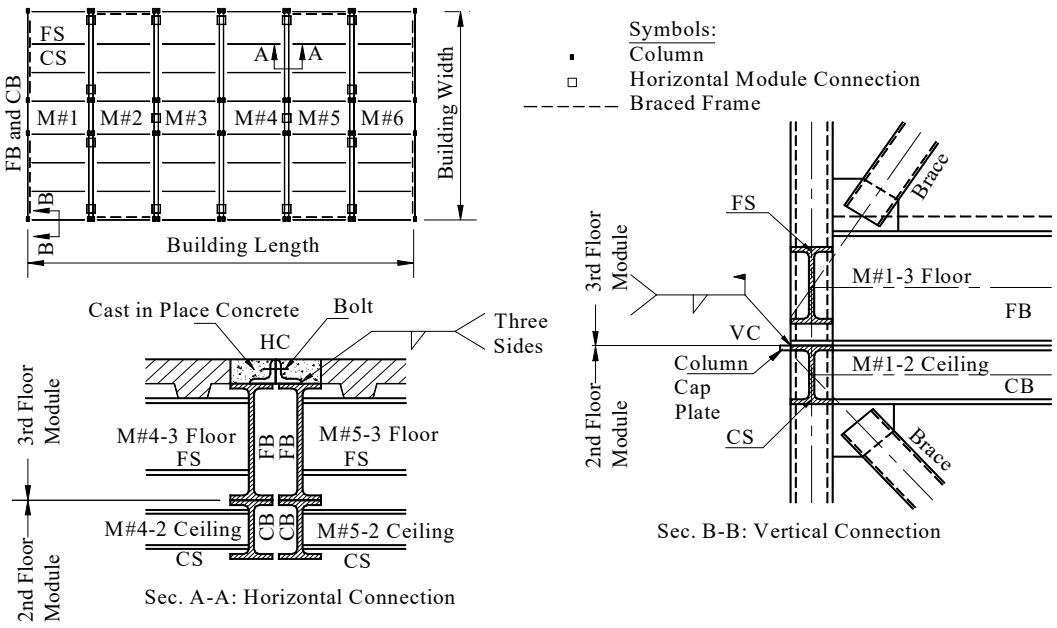

Figure 1. Typical details for a multi-story MSB

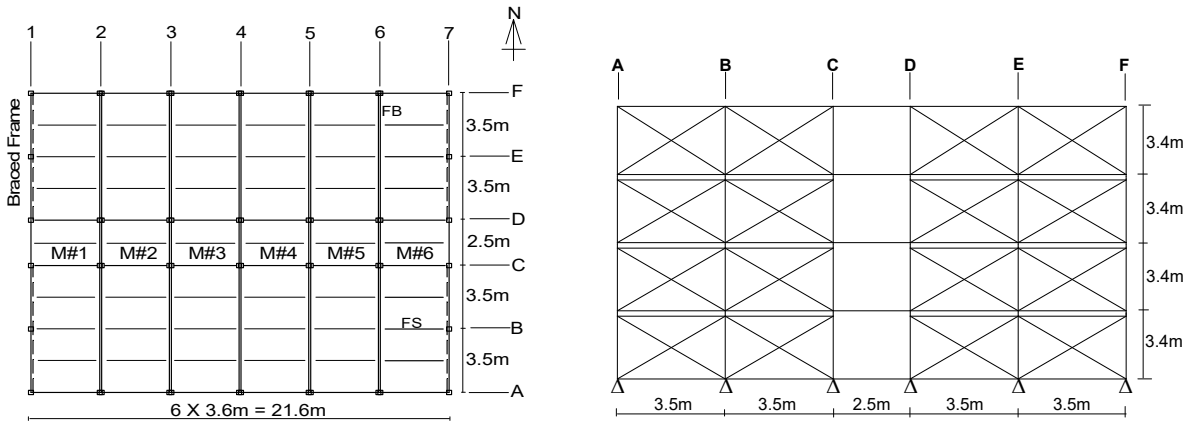

(a) (b)

Figure 2. 4-storey modular steel braced frame (a) Floor plan (b) Elevation (centerline 1 or 7)

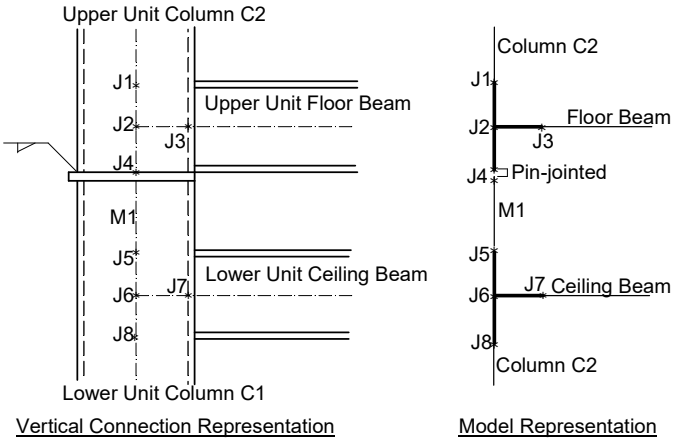

Figure 3. Model of vertical connection of modular units of MSB braced frame

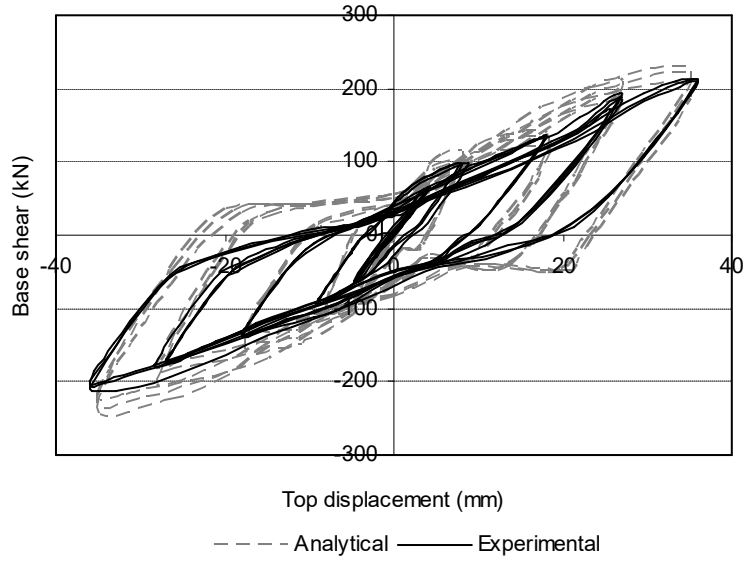

Figure 4. Comparison of experimental and analytical load-displacement curves of MSB braced specimen

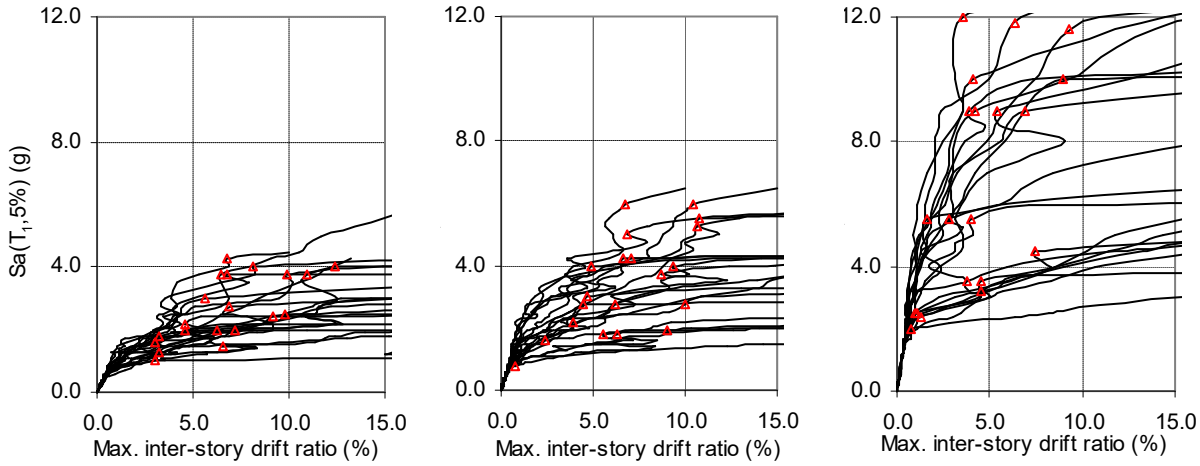

Figure 5. IDA curves of 'first mode' spectral acceleration, $S_a(T_1, 5\%)$, plotted against Max. inter-storey drift ratio, θ_{max}, for (a) 6-storey (b) 4-storey (c) 2-storey MSB braced frames.

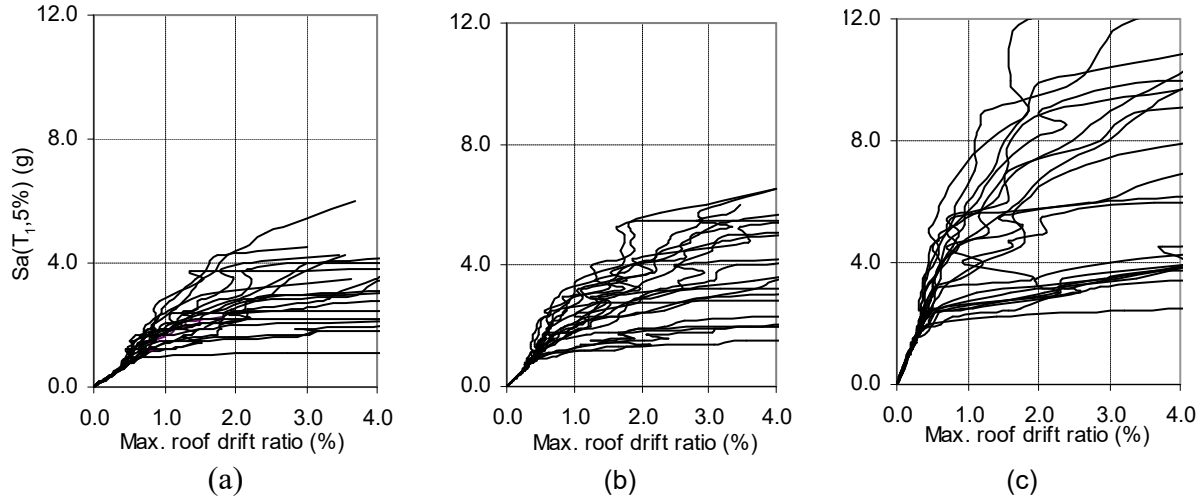

Figure 6. IDA curves of 'first mode' spectral acceleration, $S_a(T_1, 5\%)$, plotted against Peak roof drift ratio, θ_{roof}, for (a) 6-storey (b) 4-storey (c) 2-storey MSB braced frames.

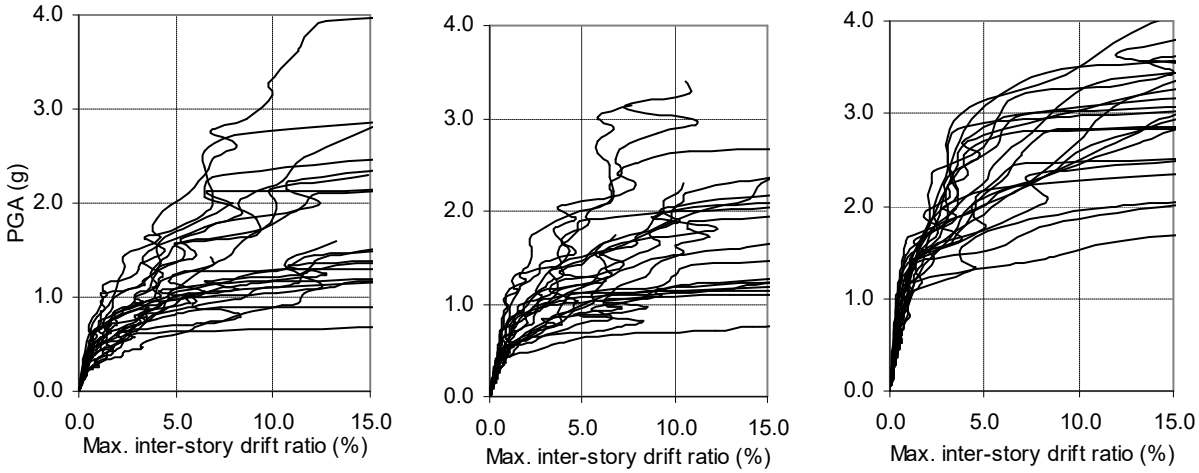

(a) (b) (c)

Figure 7. IDA curves of Peak ground acceleration, PGA, plotted against Max. Inter-storey drift ratio, θ_{max}, for (a) 6-storey (b) 4-storey (c) 2-storey MSB braced frames.

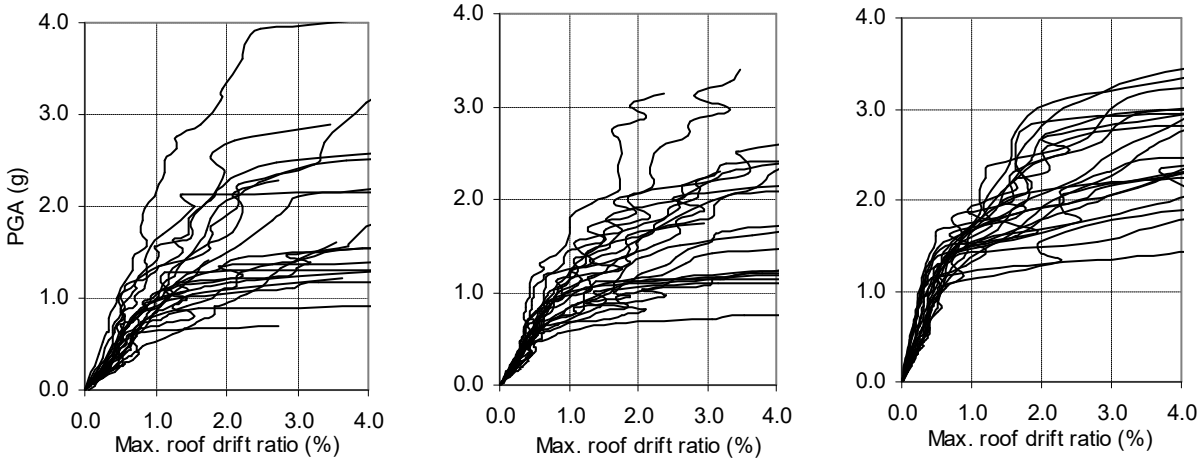

(a) (b) (c)

Figure 8. IDA curves of Peak ground acceleration, PGA, plotted against Peak roof drift ratio, θ_{roof}, for (a) 6-storey (b) 4-storey (c) 2-storey MSB braced frames.

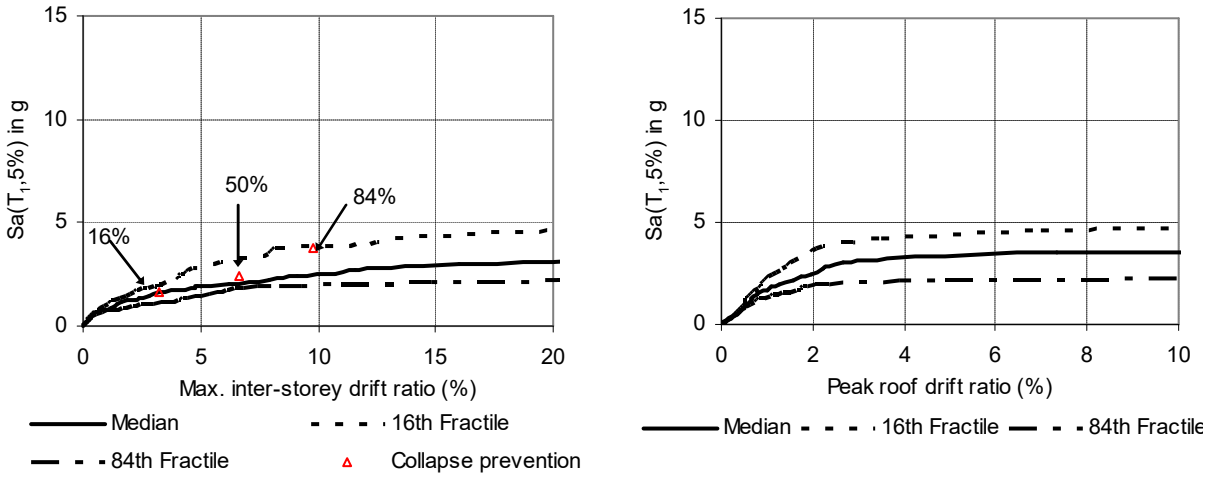

(a) (b)

Figure 9. Summary of IDA curves of the 6-storey MSB frame into16th, 50th, and 84th fractiles with (a) Max. inter-storey drift ratio (b) Peak roof drift ratio.

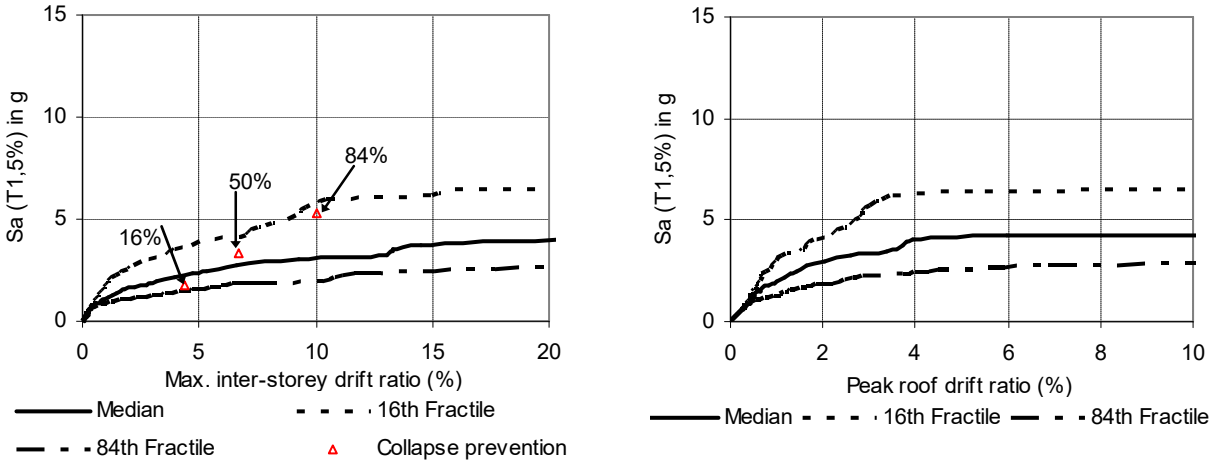

(a) (b)

Figure 10. Summary of IDA curves of the 4-storey MSB frame into16th, 50th, and 84th fractiles with (a) Max. inter-storey drift ratio (b) Peak roof drift ratio.

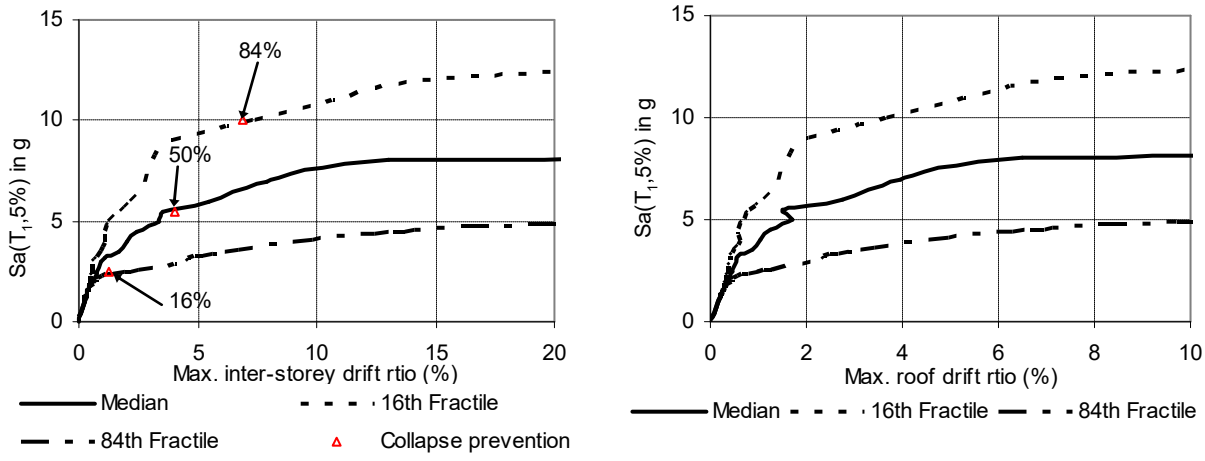

(a) (b)

Figure 11. Summary of IDA curves of the 2-storey MSB frame into16th, 50th, and 84th fractiles with (a) Max. inter-storey drift ratio (b) Peak roof drift ratio.

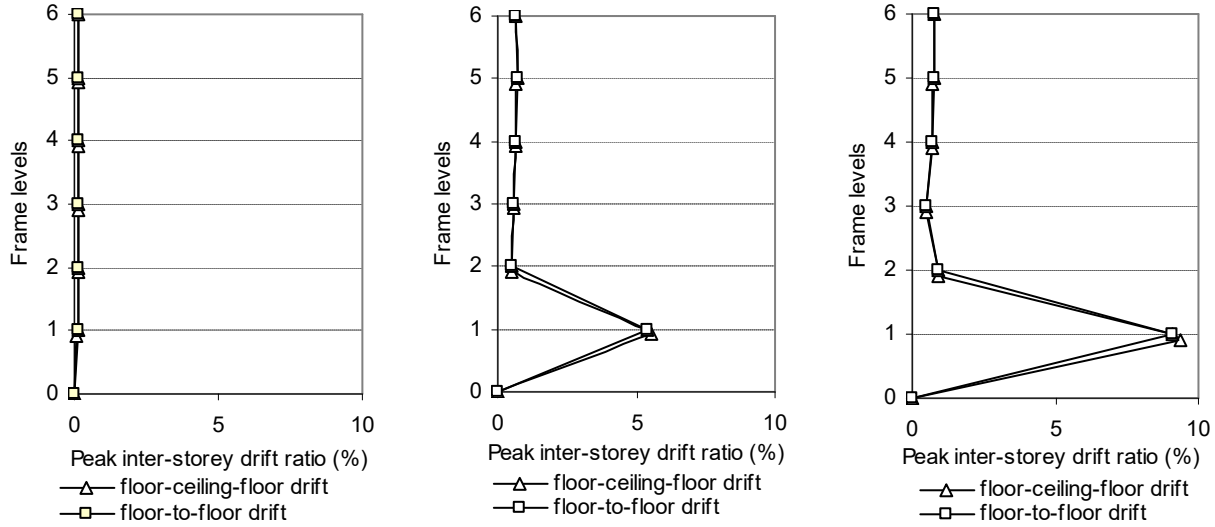

(a) (b) (c)

Figure 12. Heightwise distribution of peak inter-storey drift ratio for 6-storey MSB (a) $S_a(T_1, 5\%) = 0.2g$ (b) $S_a(T_1, 5\%) = 1.7g$ (c) $S_a(T_1, 5\%) = 2.0g$

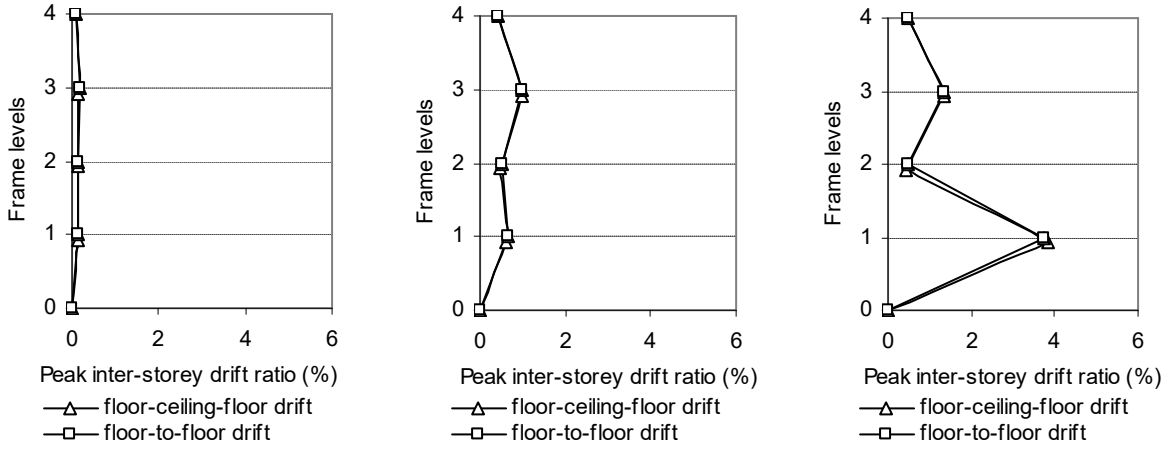

Figure 13. Heightwise distribution of peak inter-storey drift ratio for 4-storey MSB (a) $S_a(T_1, 5\%) = 0.3g$ (c) $S_a(T_1, 5\%) = 2.0g$ (d) $S_a(T_1, 5\%) = 3.0g$

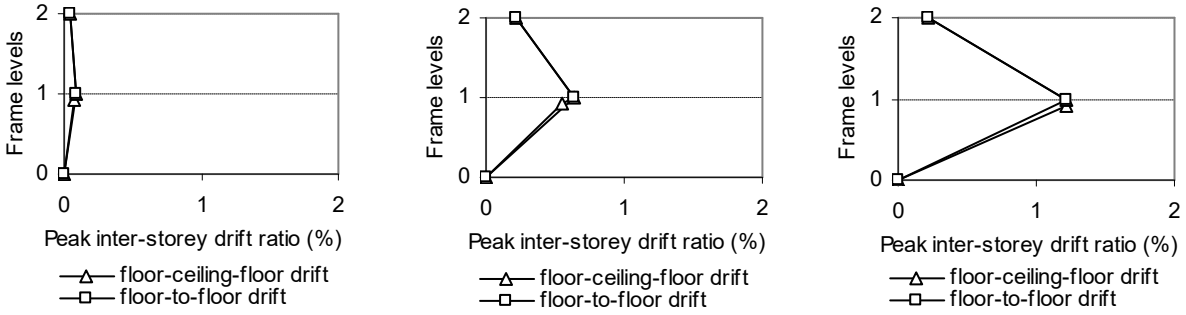

Figure 14. Heightwise distribution of peak inter-storey drift ratio for 2-storey MSB (a) $S_a(T_1, 5\%) = 0.4g$ (b) $S_a(T_1, 5\%) = 2.5g$ (c) $S_a(T_1, 5\%) = 4.0g$

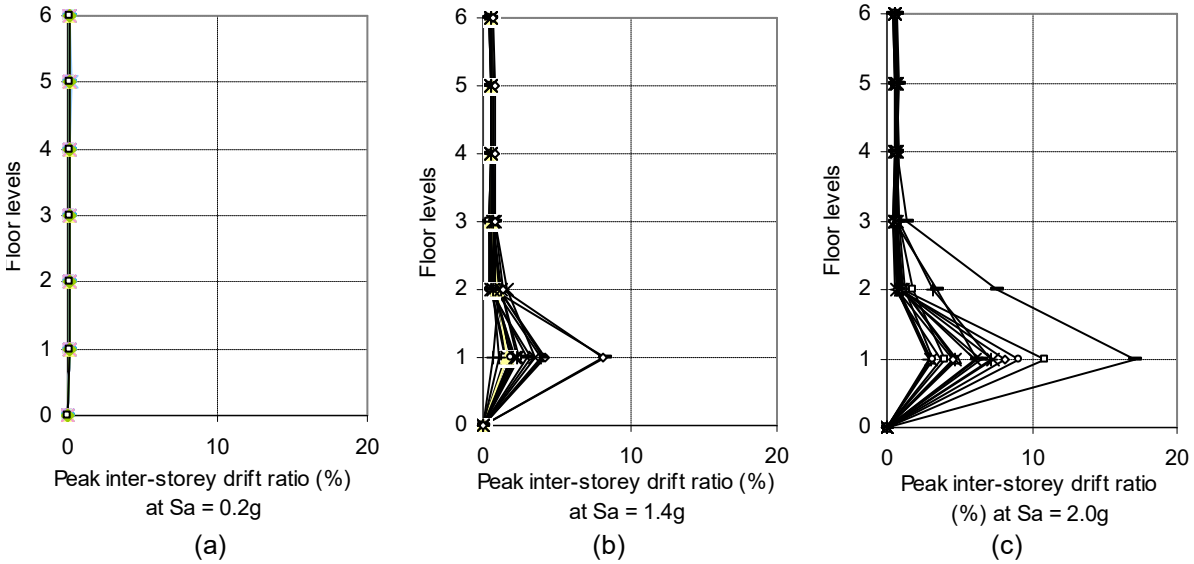

Figure 15. Peak inter-storey drift along height of 6-storey MSB frame under selected ground motion records at different intensity levels (a) $S_a = 0.2g$ (b) $S_a = 1.4g$ (c) $S_a = 2.0g$

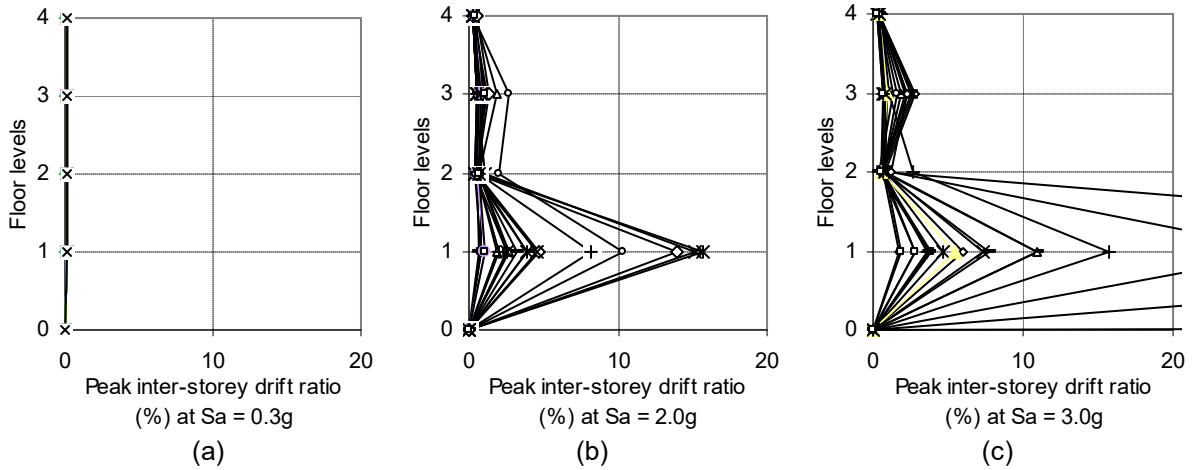

Figure 16. Peak inter-storey drift along height of 4-storey MSB frame under selected ground motion records at different intensity levels (a) S_a = 0.3g (b) S_a = 2.0g (c) S_a = 3.0g

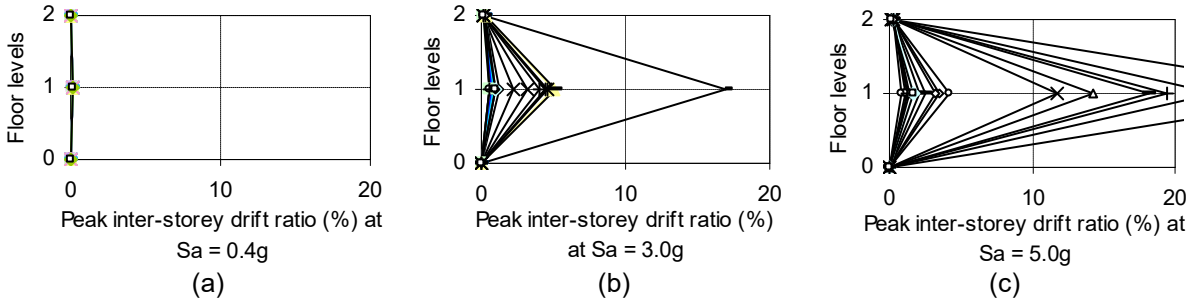

Figure 17. Peak inter-storey drift along height of 2-storey MSB frame under selected ground motion records at different intensity levels (a) Sa = 0.4g (b) Sa = 3.0g (c) Sa = 5.0g

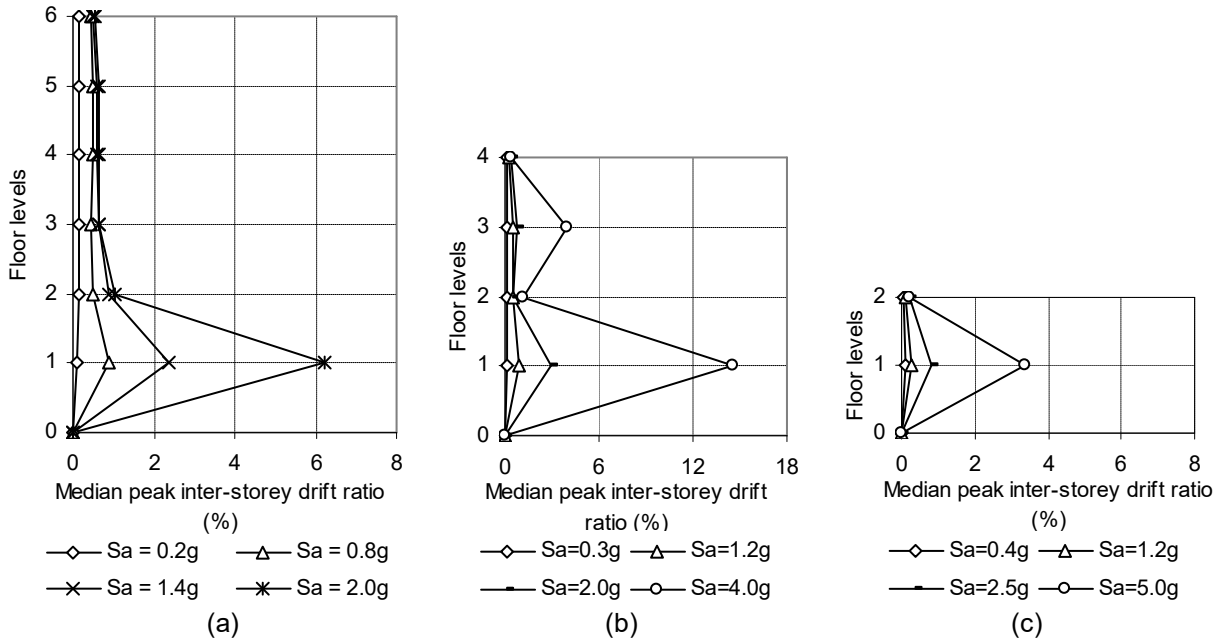

Figure 18. Median peak inter-storey drift ratios for all storey levels at different ground motion intensities representing elastic and post-elastic response (a) 6-storey (b) 4-storey (c) 2-storey

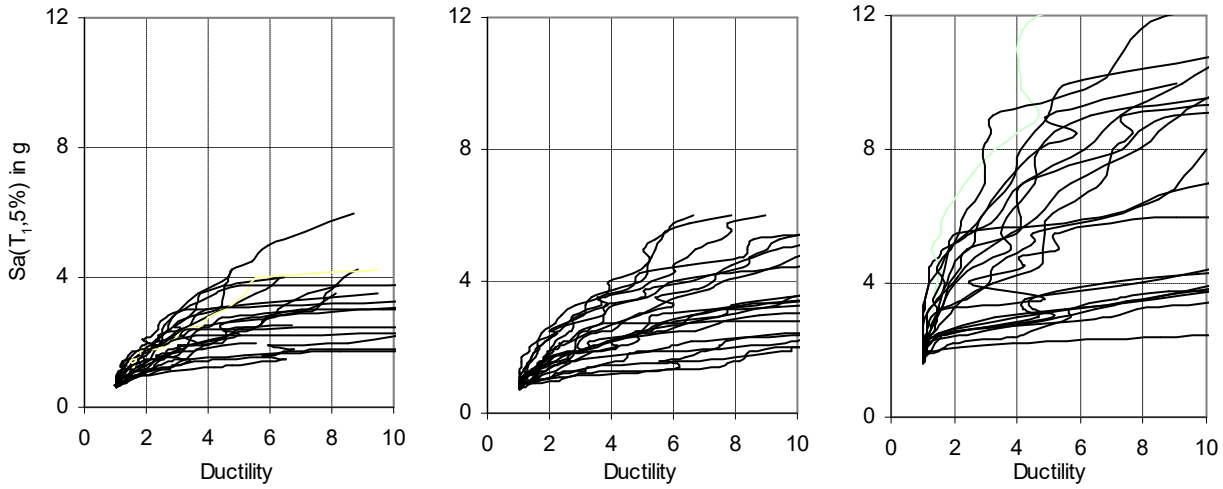

Figure 19. IDA curves of 5% damped spectral acceleration, $S_a(T_1, 5\%)$, plotted against ductility for (a) 6-storey (b) 4-storey (c) 2-storey MSB braced frames.

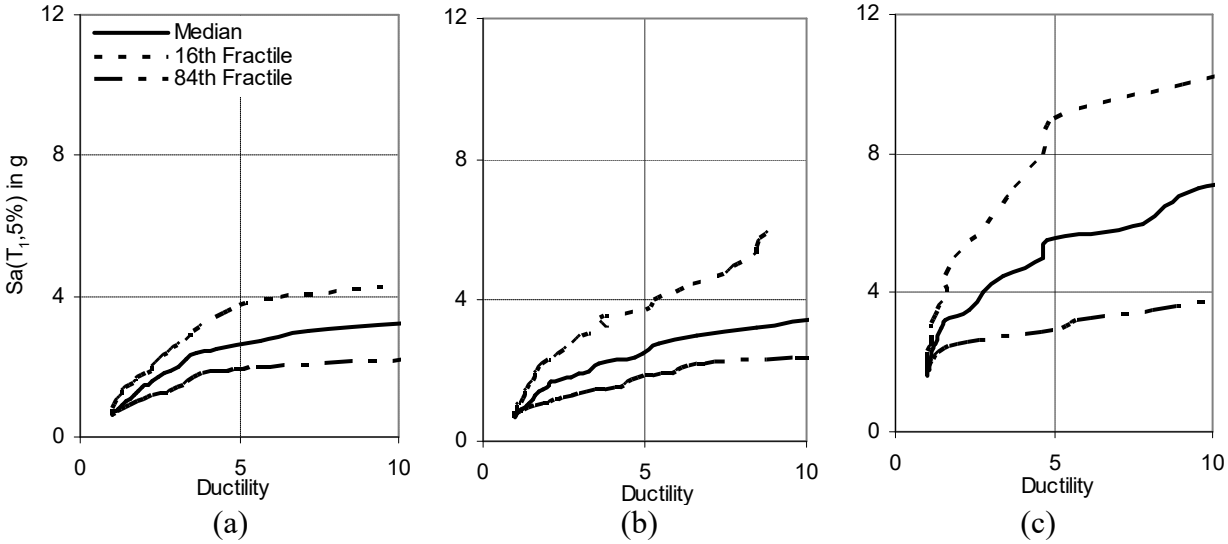

Figure 20. Summary of ductility demand IDA curves into 16th, 50th, and 84th fractiles for (a) 6-storey (b) 4-storey (c) 2-storey MSB frames.